Low activation energy dehydrogenation of aqueous formic acid on platinum–ruthenium–bismuth oxide at near ambient temperature and pressure†

Siu-Wa Ting, Shaoan Cheng,‡ Kwok-Ying Tsang, Nicole van der Laak and Kwong-Yu Chan*

Received (in Cambridge, UK) 11th August 2009, Accepted 12th October 2009
First published as an Advance Article on the web 22nd October 2009
DOI: 10.1039/b916507j

Highly selective dehydrogenation of formic acid in water was observed at near ambient temperature on a metal/metal oxide catalyst composed of platinum ruthenium and bismuth with a low activation energy of 37.3 kJ mol^{-1}.

Formic acid decomposition has been investigated over the decades[1–20] using catalysts of metals,[2,5–7] metal oxides,[8–13] and metal supported on oxides.[14–20] The reaction can also proceed without catalysts under hydrothermal conditions[21–23] to temperatures of 280–330 °C and a pressure of 275 bar. Recent studies have been motivated by the interest of generating hydrogen to feed fuel cells[24,25] and lowering the temperature of the water–gas-shift process.[16–19] Most previous studies have been made at an elevated temperature and with gaseous reactants and products. A gas phase reaction will require heating above 100 °C, the normal boiling point of formic acid, or pulling a vacuum, or introducing an inert carrier gas to dilute formic acid below its saturated vapor pressure. These constraints would add complexity to a hydrogen generation device. A few recent studies have focused on a selective dehydrogenation reaction in the liquid phase at near ambient temperature.[24–32] Selective dehydrogenation of aqueous formic acid at near ambient temperature was observed with soluble metal complexes of ruthenium[25,27–31] and rhodium.[24,26] An inert atmosphere[27–31] and the presence of an amine may be required.[29–31] It is desirable to have an insoluble catalyst for fixed bed flow-through operations and that excess water from aqueous formic acid feed can be removed without draining the catalyst. The recent report of Pd–Au and Pd–Ag catalysts shows good decomposition rates at near ambient temperature.[32] Kinetically, the dehydrogenation reaction is favored in the presence of a metal catalyst such as platinum, which is thought to catalyze the C–H bond cleavage. It is well known in fuel cell literature that ruthenium acts as a CO tolerant co-catalyst to platinum,[33,34] whereas a bimetallic PtBi catalyst was shown to have good activity for electrooxidation of formic acid to CO_2.[35–37] The enhanced activity is suggested to be caused by a change of lattice spacing in PtBi which reduces CO affinity.[35] The other suggestion is the promoted oxidation of adsorbed CO by OH preferentially adsorbed on Bi.[37] Previous investigations of formic acid decomposition have been mostly made with a single metal or metal supported on a metal oxide which may not be sufficiently selective or still possesses a high activation energy barrier. Studies of bimetallic catalysts have not been reported until very recently[32] and there have also been no studies of bismuth or bismuth oxide. We report here, for the first time, a bismuth containing catalyst composited with platinum and ruthenium. This heterogeneous catalyst decomposes formic acid in liquid water at ambient temperature with high rates, yielding exclusively hydrogen and carbon dioxide with a very low activation energy.

The catalyst can be synthesized (ESI†) with various compositions of precursors containing Pt, Ru, and Bi with bismuth in an oxidized form, and is generally denoted $PtRuBiO_x$ with ratios of the metals to be further specified. Upon contacting the $PtRuBiO_x$ catalyst at room temperature, aqueous formic acid shows steady gas evolution. The product gas was continuously analyzed and contained equi-molar hydrogen and carbon dioxide without detection of carbon monoxide (Table S1 and Fig. S1†). A typical 7 h gas evolution from an 80 mL 15% v/v formic acid in water immersed with 400 mg catalyst of 30% metal loaded carbon is shown in Fig. 1. The rate of gas generation is initially high but decreased gradually before reaching steady-state after 1 h. This apparent deactivation can be explained by product CO_2 occupation of catalyst active sites which were initailly all available for formic acid decomposition. The forward rate of CO_2(ad) to CO_2(aq)

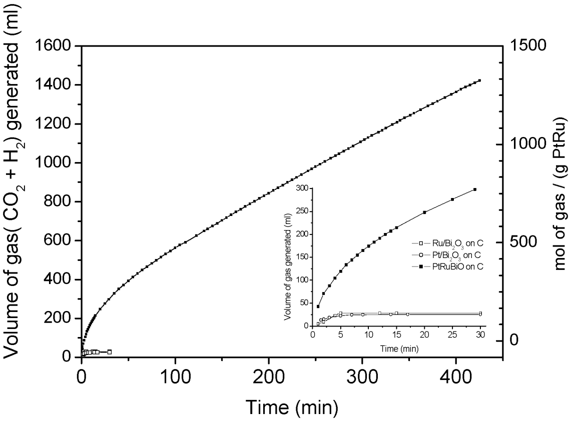

Fig. 1 Decomposition of formic acid on Pt–Ru–BiO_x/C (Pt/Ru/Bi ~ 2 : 1 : 4) at 80 °C over 7 h. Inset: activity of initial 30 min for better comparison with Pt–Bi_2O_3 /C and Ru–Bi_2O_3/C.

Department of Chemistry, The University of Hong Kong,
Pokfulam Road, Hong Kong SAR, P.R. China.
E-mail: hrsccky@hku.hk; Fax: +852 28571586

† Electronic supplementary information (ESI) available: Experimental details and supporting information. See DOI: 10.1039/b916507j

‡ Present address of Shaoan Cheng: State Key Laboratory of Clean Energy Utilization, Zhejiang University, Hangzhou, China 310027.

to CO_2(gas) is gradually balanced by a backward rate at steady-state.

The typically synthesized $PtRuBiO_x$ catalyst is comprised of nanoparticles with an average size of 5 nm supported on Vulcan XC-72 carbon as shown in Fig. 2 and Fig. S2.† At a fixed concentration and volume of aqueous formic acid, the decomposition rate increased linearly with catalyst mass (Fig. S3†) and can be scaled to precious metal content as 1.3 mol/(g of PtRu) over the 7 h period in Fig. 1. Over a much longer time interval, gas evolution will decline unless formic acid is replenished to compensate for its consumption. For different compositions of $PtRuBiO_x$ catalyst used, a varying degree of reactivity was found as shown by the initial as well as steady-state rates in Table S2.† The initial rates on different catalysts vary between 0.57 to 2.65 times of the initial rate shown in Fig. 1. Metal dispersion was estimated using TEM particle size distribution shown in Fig. S3.† Based on Pt and Ru surface atoms, the turn over frequency (TOF) was estimated to be 312 h^{-1} in the first hour of the decomposition shown in Fig. 1. Bismuth oxide is not acting as a support since no activity was found in PtRu supported on carbon or titanium dioxide or alumina. Bismuth oxide plays an enabling role for the ambient temperature reaction as control experiments using a single metal of Pt and Ru, Bi, their oxides, binary metal mixture and oxides all show no activity except $PtBiO_x$ and $RuBiO_x$. The activity of the last two binary mixtures with bismuth are, however, very low compared to the $PtRuBiO_x$, as shown in Fig. 1. The oxidation state of bismuth was determined by XPS to be exclusively +3, whereas appreciable amounts of Pt and Ru are in oxides or hydroxide (Fig. S4†). The bismuth content and state in the used catalysts was analyzed to be unchanged.

Initial reaction rates determined over the range of 40–90 °C yields a linear inverse temperature plot with an activation energy of 37.3 kJ mol^{-1} as shown in Fig. 3. This value is lower than all previously reported values except that on a mixture of chromium oxide and potassium oxide.[12] Most reported activation energies for both dehydrogenation and dehydration for formic acid are >100 kJ mol^{-1},[1,12] with a few reported values between 40 to 90 kJ mol^{-1}.[20,24,26] The apparent lower activation energy may be attributed to thermodynamic and kinetic factors in the aqueous environment using the specific catalyst including the efficiency of PtRu for CO resistant C–H cleavage; and the lower enthalpy value of CO_2 dissolved in water or adsorbed on the basic Bi_2O_3. Both dehydrogenation (I) and dehydration (II) are mildly endothermic as shown by their standard enthalpies of reactions at 25 °C with

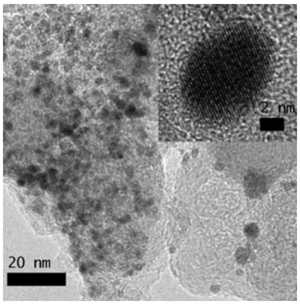

Fig. 2 Transmission electron microscopy image of the $PtRuBiO_x$ catalyst used for the reaction shown in Fig. 1.

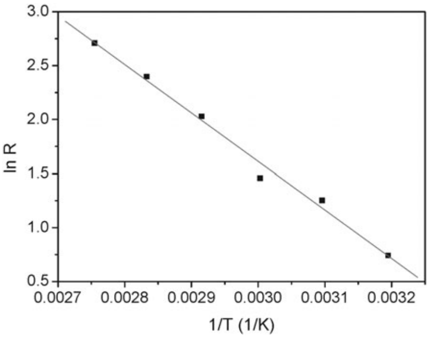

Fig. 3 An Arrhenius plot for the HCOOH decomposition on $PtRuBiO_x$/C.

$$HCOOH(l) \rightarrow CO_2(g) + H_2(g)\ \Delta_rH^\circ = 31.2\ \text{kJ mol}^{-1}, \quad (I)$$

$$\text{and } HCOOH(l) \rightarrow CO(g) + H_2O(l)\ \Delta_rH^\circ = 28.4\ \text{kJ mol}^{-1}. \quad (II)$$

Dehydration becomes more endothermic (an additional 44 kJ mol^{-1}) when water produced is gaseous.[39] On the other hand, dissolved CO_2(aq) in liquid phase can lower the enthalpy of dehydrogenation by 20.3 kJ mol^{-1}. Experimental results[19,22,22] showed higher selectivity towards CO_2 generation under hydrothermal conditions, suggesting a possible thermodynamic enhancement. The possible lower activation energy of dehydrogenation of formic acid in water has also been investigated theoretically.[40]

The reaction rate is sensitive to the concentration of formic acid in water with a maximum rate at *ca.* 15% v/v or 3 M, as shown in Fig. 4. This optimum concentration is consistent with the concentration used by Laurenczy and co-workers.[27,28] Concentrations of molecular formic acid and formate ion change interactively with changing concentration of the formic acid/water mixture. Detailed potentiometric titration studies[41] show maximum formic acid dissociation in the range of 25–65 wt% HCOOH in water with a max $HCOO^-$ concentration of 0.07 M. The rate dependence in Fig. 4 can therefore be interpreted as an effect of concentration of one or both of HCOOH, $HCOO^-$ and to a minor extent water at high concentration of formic acid. Recent reports of aqueous formic acid decomposition have all used a mixture of formic acid/sodium formate with a definite ratio.[27,28,32] In our experiments using the $PtRuBiO_x$ catalyst, the decomposition rate is linearly dependent on formic acid concentration when the formate ion is in excess (Fig. S6).† It is also linearly dependent on formate ion concentration when formic acid is in excess (Fig. S7).† The reaction can therefore be bimolecular in nature and depends on both HCOOH and $HCOO^-$ concentrations. Borowiak *et al.* have discussed the bimolecular HCOOH/$HCOO^-$ mechanism giving higher selectivity towards dehydrogenation.[42] Through *ab initio* calculations of activation complexes with a few water molecules present, Akiya and Savage[40] showed the role of water in lowering the activation energy for the dehydrogenation path. Hence the reaction mechanism may involve a combination of water, molecular formic acid, and formate ion.

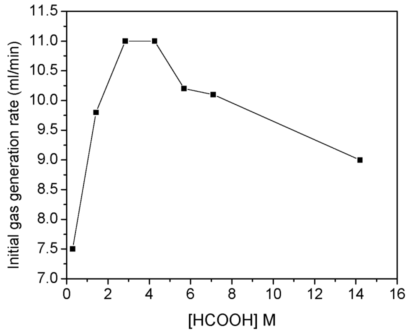

Fig. 4 The initial rate of Pt/Ru/BiO on Vulcan-72 carbon (Pt/Ru/Bi ~ 2 : 1 : 4) towards formic acid decomposition at 80 °C with different concentrations of formic acid.

The high selectivity and high rate may be attributed to the synergistic roles of platinum, ruthenium, and bismuth oxide in cleaving C–H bonds, minimizing CO adsorption or oxidizing CO, and facilitating generation and removal of CO_2. Chemisorption measurements showed significantly less CO sorption on $PtRuBiO_x$ than PtRu on Vulcan carbon (see ESI Part 7†). The role of Ru in promoting Pt for efficient C–H cleavage without CO poisoning has been discussed[33,34] and a similar role has been suggested for Bi.[35–37] Bismuth oxide appears to offer a unique role in lowering the activation energy and offering high selectivity to dehydrogenation. Bismuth has different carbonates including $(BiO)_4(OH)CO_3$ and bismuth subcarbonate $(BiO)_2(CO_3)$ that can be formed from CO_2, water, and Bi_2O_3[38] and play a possible role in removing the product or forming the intermediate as adsorbed CO_2.

The high selectivity and high reaction rate of the $PtRuBiO_x$ catalyst at ambient conditions show promise for a convenient hydrogen generation device. Further increase in reaction rates is possible with a continuous flow-through reactor packed with the heterogeneous catalyst. Optimizations can be made in fine tuning catalyst composition, particle size, properties of the support, and operation pressure. The low activation energy of the reaction and the unique role of bismuth oxide suggest new perspectives in the mechanisms of formic acid dehydrogenation in the aqueous phase.

Financial support from The Hong Kong Research Grants Council GRF HKU 700208P, "Initiative on Clean Energy and Environment" of The University of Hong Kong Development Fund, and the HKU Strategic Research Theme on "Clean Energy Research" are acknowledged.

Notes and references

1 A. Mailhe and P. Sabatier, *Compt. Rend. Acad. Sci.*, 1911, **152**, 1212.
2 K. Hirota, K. Kuwata and Y. Nakai, *Bull. Chem. Soc. Jpn.*, 1958, **31**, 861.
3 P. Mars, *Proceedings of symposium on the mechanism of heterogeneous catalysis*, Amsterdam, The Netherlands, 1959.
4 P. Mars, J. J. F. Scholten and P. Zwietering, *Adv. Catal.*, 1963, **14**, 35.
5 Y. K. Sun, J. J. Vajo, C. Y. Chan and W. H. Weinberg, *J. Vac. Sci. Technol., A*, 1988, **6**, 854.
6 D. H. S. Ying and R. J. Madix, *J. Catal.*, 1980, **61**, 48.
7 N. Aas, Y. Li and M. Bowker, *J. Phys.: Condens. Matter*, 1991, **3**, S281.
8 X. D. Peng and M. A. Barteau, *Catal. Lett.*, 1991, **7**, 395.
9 P. A. Dilara and J. M. Vohs, *J. Phys. Chem.*, 1993, **97**, 12919.
10 V. A. Gercher and D. F. Cox, *Surf. Sci.*, 1994, **312**, 106.
11 J. Stubenrauch, E. Brosha and J. M. Vohs, *Catal. Today*, 1996, **28**, 431.
12 R. Larsson, M. H. Jamroz and M. A. Borowiak, *J. Mol. Catal. A: Chem.*, 1998, **129**, 41.
13 G. Y. Popova, T. V. Andrushkevich, Y. A. Chesalov and E. S. Stoyanov, *Kinet. Catal.*, 2000, **41**, 805.
14 A. Bandara, J. Kubota and A. Wada, *J. Phys. Chem. B*, 1997, **101**, 361.
15 J. Rasko, T. Kecskes and J. Kiss, *J. Catal.*, 2004, **224**, 261.
16 T. Shido and Y. Iwasawa, *J. Catal.*, 1993, **141**, 71.
17 G. Jacobs, P. M. Patterson, U. M. Graham, A. C. Crawford and B. H. Davis, *Int. J. Hydrogen Energy*, 2005, **30**, 1265.
18 G. Jacobs, P. M. Patterson, U. M. Graham, A. C. Crawford, A. Dozier and B. H. Davis, *J. Catal.*, 2005, **235**, 79.
19 Y. Yasaka, H. Yoshida, C. Wakai, N. Matubayasi and M. Nakahar, *J. Phys. Chem. A*, 2006, **110**, 11082.
20 M. Ojeda and E. Iglesia, *Angew. Chem., Int. Ed.*, 2009, **48**, 4800.
21 A. Bjerre and E. Sorensen, *Ind. Eng. Chem. Res.*, 1992, **31**, 1574.
22 J. Yu and P. E. Savage, *Ind. Eng. Chem. Res.*, 1998, **37**, 2.
23 P. G. Maiella and T. B. Brill, *J. Phys. Chem. A*, 1998, **102**, 5886.
24 S. Fukuzumi, T. Suenobu and S. Ogo, WO/2008/059630, PCT/JP2007/060115.
25 G. Laurenczy, C. Fellay and P. Dyson, WO/2008/047312, PCT/IB2007/054222.
26 S. Fukuzumi, T. Kobayashi and T. Suenobu, *ChemSusChem*, 2008, **1**, 827.
27 C. Fellay, P. J. Dyson and G. Laurenczy, *Angew. Chem., Int. Ed.*, 2008, **47**, 3966.
28 C. Fellay, N. Yan, P. J. Dyson and G. Laurenczy, *Chem.–Eur. J.*, 2009, **15**, 3752.
29 B. Loges, A. Boddien, H. Junge and M. Beller, *Angew. Chem., Int. Ed.*, 2008, **47**, 3962.
30 H. Junge, A. Boddien, F. Capitta, B. Loges, J. R. Noyes, S. Gladiali and M. Beller, *Tetrahedron Lett.*, 2009, **50**, 1603.
31 A. Boddien, B. Loges, H. Junge and M. Beller, *ChemSusChem*, 2008, **1**, 751.
32 X. Zhou, Y. Huang, W. Xing, C. Liu, J. Liao and T. Lu, *Chem. Commun.*, 2008, 3540.
33 M. Watanabe, M. Uchia and S. Motto, *J. Electroanal. Chem.*, 1987, **229**, 395.
34 H. Schmidt, P. Buchner, A. Datz, K. Dennerlein, S. Lang and M. Waidbas, *J. Power Sources*, 2002, **105**, 243.
35 E. Casado-Rivera, Z. Gal, A. C. D. Angelo, C. Lind, F. J. DiSalvo and H. D. Abruna, *ChemPhysChem*, 2003, **4**, 193.
36 E. Casado-Rivera, D. Volpe, L. Alden, C. Lind, C. Downie, T. Vazquez-Alvarez, A. C. D. Angelo, F. J. DiSalvo and H. D. Abruna, *J. Am. Chem. Soc.*, 2004, **126**, 4043.
37 A. V. Tripkovic, K. Dj. Popovic, R. M. Stevanovic, R. Socha and A. Kowal, *Electrochem. Commun.*, 2006, **8**, 1492.
38 P. Taylor, S. Sunder and V. J. Lopata, *Can. J. Chem.*, 1984, **62**, 2863.
39 I. Martin, T. Skalicky, J. Langer, H. Abdoul-Carime, G. Karwasz, E. Illenberger, M. Stano and S. Matejcik, *Phys. Chem. Chem. Phys.*, 2005, **7**, 2212.
40 N. Akiya and P. E. Savage, *AIChE J.*, 1998, **44**, 405.
41 J. S. Ferrer, E. Couallier, M. Rakib and G. Durand, *Electrochim. Acta*, 2007, **52**, 5773.
42 M. A. Borowiak, M. H. Jamróz and R. Larsson, *J. Mol. Catal. A: Chem.*, 2000, **152**, 121.